Journal of Mathematical Chemistry 25 (1999) 321–344

Discretization of unknown functions: A new method to solve partial differential equations with mixed boundary conditions

A. Grassi [a], G.M. Lombardo [a] and A. Raudino [b]

[a] *Dipartimento di Scienze Chimiche, Facoltà di Farmacia, Università di Catania, V. le A. Doria 6, 95125 Catania, Italy*

[b] *Dipartimento di Scienze Chimiche, Facoltà di Scienze Mat. Fis. & Nat., Università di Catania, V. le A. Doria 6, 95125 Catania, Italy*

Received 21 September 1998; revised 13 May 1999

In this paper, we develop a new numerical technique to obtain an approximate solution of partial differential equations subject to mixed boundary conditions (MBCs). The approach has been applied to a class of differential equations which frequently arise in a large variety of problems such as heat conduction, potential theory, and diffusion-controlled chemical reactions. In our approach, based on the discretization of unknown functions (DF), the solution is expressed as a series expansion and the determination of the series coefficients is reduced to the solution of a system of algebraic equations. The main advantages of the DF procedure are: (a) the smoothness of the function and of its first derivative in the different domains, whereas the other numerical methods generally show a highly oscillating behavior; (b) the fast convergence of the series expansion. This method has been applied to solve diffusion problems in different coordinate systems (trigonometric, cylindrical and spherical). The obtained results have been compared with the analytical solution (when available) as well as with other numerical methods commonly used to solve MBCs problems.

0. Introduction

Mixed boundary conditions (MBC) frequently arise in various areas of chemistry, physics and biology. A typical example of mixed boundary problem is the diffusion of reactant through the intercellular solution and the subsequent reaction with a receptor located at the cell membrane surface. Being the receptors located in restricted areas of the membrane surface, the reactants are adsorbed inside these areas and reflected outside, as schematically depicted in figure 1. Several studies devoted to this topic have been performed by our [2–8,15] and other groups [1,12,21,28,30,31,36,37,39]. Potential theory is another area where mixed boundary problems frequently arise. One of the simplest problems we can conceive in electrostatics is that of calculating the electrostatic potential of a circular disk which is charged to a fixed potential. The continuity condition and the constancy of the potential on the disk impose that the

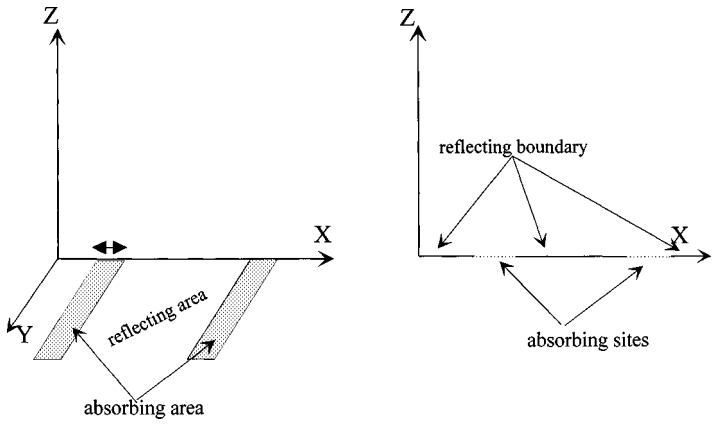

Figure 1. Schematic representation of the mixed boundary conditions for the diffusion equation (equation (1) in the main text). (a) Three-dimensional case; (b) two-dimensional case.

derivative of the potential on the disk is proportional to the charge density. The solution of the problem requires solving Laplace's equation subject to MBCs. This latter problem and many others taken from the potential theory have been widely treated in the book of Sneddon [29]. Finally, heat conduction in a plate whose top surface is both partially insulated and partially exposed to a fluid medium is another example of a mixed boundary value problem [11,18]. These are just only a few examples; we refer to the specialized literature for a full discussion of physical problems which lead to MBCs [10,13,20,22,27].

A general mixed boundary problem can be written as follows. Let

$$L(f) = \nabla^2 f - g(\mathbf{x}) f = 0, \quad \forall \mathbf{x} \in R, \tag{1}$$

be a generic second-order PDE (partial differential equation) defined into domain R, where $f = f(\mathbf{x})$ and $\mathbf{x} = (x_1, x_2, x_3)$.

The mixed boundary conditions of equation (1) can be represented as

$$f(x_1, x_2, 0) = w_1(x_1, x_2, 0), \quad \forall (x_1, x_2) \in D_A, \tag{2a}$$

$$\nabla f(x_1, x_2, x_3)|_{x_3=0} = w_2(x_1, x_2, 0), \quad \forall (x_1, x_2) \in D_B, \tag{2b}$$

where $D \equiv D_A \cup D_B$. Moreover, $w_1(\mathbf{x})$ and $w_2(\mathbf{x})$ are generic prescribed functions.

The general solution of equation (1) can be often expressed in terms of an infinite series consisting of products of functions, which are solutions of equation (1), multiplied for undermined coefficients. If one applies the boundary conditions (2a) and (2b), a pair of so-called dual-series equations is obtained from which the coefficients can be calculated. Unfortunately, the analytical solution of the pair of dual series equations is known in all but a few cases, depending on the analytical structure of the $w_i(\mathbf{x})$ functions in equation (2). On the contrary, several approximate analytical, as well as purely numerical techniques, are available to solve dual-series equations,

for instance, finite difference methods [35], artificial interface techniques [17,38] or weighted residual methods (MWR) [14,32–34,40].

Generally, purely numerical techniques show two disadvantages: (a) the solution is not obtained in a closed form; (b) there is the need of small mesh sizes near the discontinuity region at the D_A, D_B boundary, in order to achieve some degree of accuracy. These circumstances produce a computational effort, especially in two- or three-dimensional PDEs, as it will be discussed in the next section.

Among the approximate analytical methods we mention the artificial interface method (AIM), first proposed by Wilson [38], where an artificial interface is introduced at the boundary separating the D_A and D_B regions. The solutions found in both regions are matched at the artificial interface in order to find the series coefficients. As pointed out by Mills and Dudukovic [13], this method is often not satisfactory for problems in cylindrical or spherical coordinates.

Some years ago, Mills and Dudukovic [13,22–26] in a interesting series of papers have compared different approximate analytical techniques, based on the weighted residual method, with the above mentioned AIM methods as well as with the exact analytical solution (when available). In particular, they compared the solutions of mixed boundary value problems for different series including trigonometric, Bessel's cylindrical and Legendre's spherical functions. The MWR techniques, which embody Galerkin, collocation points and least-square methods, show a satisfactory accuracy in reproducing the MBCs in all the coordinates systems, and, in particular the least-square method (LS) seems to be the most accurate among the MWR techniques.

In this paper we compare the MWR methods with another approach developed by us and based on the discretization of two unknown functions (DF) which are the solutions of the MBCs into the two D_A and D_B sub-domains. This method has some resemblance with the AIM technique, but the procedure to obtain the series coefficients is completely different.

In section 2 we develop the MWR and DF methods, and in section 3 we apply these techniques to find the solution of a MBCs problem which arises from a simple diffusion equation. This problem has been solved in trigonometric, cylindrical and spherical coordinates in order to compare the efficiency of the DF method in different coordinates.

Here we anticipate that the results obtained by the DF method are comparable in all coordinate systems with those found by the MWR methods as well as with the analytical solution (which, for the cases where it is known, in always expressed as a slowly converging series). The main advantage of our DF method, when compared with the others, is the smoothness of the derivative function throughout the entire domain, where the other methods show an highly oscillating behavior (especially in the D_A domain), even by inserting a large number of terms in the series expansion. Therefore, in section 4 we will demonstrate that the DF method well reproduces mixed boundary conditions and that it is a useful and rapid approach when the analytical solution is lacking.

1. The convergence problem

Let us discuss in more detail the usefulness for a rapid converging series representation of MBCs solution.

Consider, for instance, the problem of calculating the diffusion controlled chemical kinetics onto a patterned surface consisting of an ordered array of reactive (receptors) and inert regions as discussed in the introduction. When the freely diffusing chemical substance (treated either as a point-like particle or as a rigid body undergoing rotational and translation Brownian motion) impinges at the receptor site is destroyed (or chemical transformed), otherwise it is reflected. Let d be the dimension of the diffusion equation and $X_1, X_2, \ldots, X_d$ the variables (including time), it is easy to prove that for this MBCs problem the concentration C of the diffusing particles can be always expressed by a converging series:

$$C(X_1, X_2, \ldots, X_d) = \sum_{m_1}^{\infty} \sum_{m_2}^{\infty} \cdots \sum_{m_{d-1}}^{\infty} A_{m_1,m_2,\ldots,m_{d-1}} f(X_1, X_2, \ldots, X_d), \qquad (3)$$

where $f(X_1, X_2, \ldots, X_d)$ is a solution of equation (1) and is a function of the d coordinates. In all the available solution methods, the coefficients $A_{m_1,m_2,\ldots,m_{d-1}}$ are obtained by solving a system of linear algebraic equations. For practical reasons only a limited number N of coefficients are calculated because it can be easily shown that the size of the matrix associated to the equation system grows with d as

$$n = N^{2(d-1)} \qquad (4)$$

with n the number of matrix elements. Let us estimate n for the diffusion problem discussed above. Considering only the translational diffusion motion, limiting the analysis to the steady state case ($\partial C/\partial t = 0$) and assuming a circular shape for the adsorbing sites, it follows a two-dimensional diffusion equation in cylindrical coordinates r and z. Hence, according to equation (4), the number of matrix elements n grows as N^2. For a fast converging series, N is of the order 10, hence $n = 10^2$, but for slowly converging series, $N = 100$ say, then $n = 10^4$. In both cases, there are no technical difficulties or exceedingly large computation times for routine computers. But when one considers even the slightly more complex case of an irregularly shaped (e.g., elliptical) adsorbing site, the associated diffusion equation becomes three dimensional (r, z and ϕ). In that case, the number of matrix elements is 10^4 for $N = 10$, but reaches the astonishing value of 10^8 matrix elements for $N = 100$. Finally, if we want to explore also transient effects ($\partial C/\partial t \neq 0$) or investigate the reactant rotational motion (described by a roto-translational diffusion equation with, at least, one angular variable at the lowest approximation), the fast and slowly converging series require the handling of matrices with 10^8 and 10^{16} elements, respectively!

It is obvious than even simple physical problems involving MBCs may becomes computationally intractable unless one is able to get very fast converging series.

2. DF (discretization functions) and MWR (method of weighted residuals methods)

Let

$$\sum_n a_n \mu_{1n} \psi(x) = f_1(x), \quad \forall x \in [a,b] \equiv D_A, \tag{5a}$$

$$\sum_n a_n \mu_{2n} \psi(x) = f_2(x), \quad \forall x \in [b,c] \equiv D_B, \tag{5b}$$

be a pair of dual-series equations, with $D \equiv D_A \cup D_B$. In this case $\psi(x)$ represents a complete set of orthogonal functions in D. The two series μ_{1n} and μ_{2n} and the two function $f_1(x)$ and $f_2(x)$ in general may be entirely different in form. The general problem is to find the a_n coefficients which satisfy conditions (5a) and (5b) over D_A and D_B domains, respectively.

2.1. MWR methods

Let

$$\varepsilon(x) = \sum_n a_n \mu_n \psi_n(x) - f(x) \tag{6}$$

be the boundary residual. $\varepsilon(x)$ will be equal to zero for the set of a_n coefficients found from the exact solution. The error can be forced to zero in the average sense by setting the weighted integrals of the residual equal to zero, i.e.,

$$\langle \varepsilon | w_i \rangle = 0 = \int_{D_A} \mathrm{d}x\, \varepsilon(x) w_i(x) + \int_{D_B} \mathrm{d}x\, \varepsilon(x) w_i(x). \tag{7}$$

This task can be accomplished for by one of the following techniques.

Galerkin. In the Galerkin method, the residual of equation (6) is orthogonalized with respect to the function $\psi_m(x)$, i.e.,

$$\sum_n a_n \left[\mu_{1n} \int_{D_A} \mathrm{d}x\, \psi_n(x)\psi_m(x) + \mu_{2n} \int_{D_B} \mathrm{d}x\, \psi_n(x)\psi_m(x) \right] - \left\{ \int_{D_A} \mathrm{d}x\, f_1(x)\psi_m(x) + \int_{D_B} \mathrm{d}x\, f_2(x)\psi_m(x) \right\} = 0, \quad m = 1, \ldots, N. \tag{8}$$

Setting

$$B_{n,m} \equiv \mu_{1n} \int_{D_A} \mathrm{d}x\, \psi_n(x)\psi_m(x) + \mu_{2n} \int_{D_B} \mathrm{d}x\, \psi_n(x)\psi_m(x) \tag{9}$$

and

$$F_m \equiv \int_{D_A} \mathrm{d}x\, f_1(x)\psi_m(x) + \int_{D_B} \mathrm{d}x\, f_2(x)\psi_m(x), \tag{10}$$

one obtains a system of linear equations:

$$\sum_n B_{n,m} a_n = F_m. \tag{11}$$

The unknown coefficients a_n are obtained by solving equation (11), once the integrals (9) and (10) have been calculated.

Least-square. In the least-square method, the inner product of the residual,

$$\begin{aligned}\langle \varepsilon | \varepsilon \rangle &= \int_D \left\{ \sum_n a_n \mu_n \psi_n(x) - f(x) \right\}^2 \mathrm{d}x \\ &= \int_{D_A} \left\{ \sum_n a_n \mu_{1n} \psi_n(x) - f_1(x) \right\}^2 \mathrm{d}x \\ &\quad + \int_{D_B} \left\{ \sum_n a_n \mu_{2n} \psi_n(x) - f_2(x) \right\}^2 \mathrm{d}x, \end{aligned} \tag{12}$$

is minimized with respect to the unknown coefficients a_n, i.e.,

$$\frac{\partial \langle \varepsilon | \varepsilon \rangle}{\partial a_n} = 0. \tag{13}$$

By applying equation (13) to equation (12) one obtains

$$\begin{aligned}&\sum_n a_n \mu_{1n} \mu_{1m} \int_{D_1} \mathrm{d}x\, \psi_n(x) \psi_m(x) + \sum_n a_n \mu_{2n} \mu_{2m} \int_{D_2} \mathrm{d}x\, \psi_n(x) \psi_m(x) \\ &\quad = \mu_{1m} \int_{D_A} \mathrm{d}x\, f_1(x) \psi_m(x) + \mu_{21m} \int_{D_B} \mathrm{d}x\, f_2(x) \psi_m(x). \end{aligned} \tag{14}$$

Setting

$$B_{m,n} \equiv \mu_{1n} \mu_{1m} \int_{D_A} \mathrm{d}x\, \psi_n(x) \psi_m(x) + \mu_{2n} \mu_{2m} \int_{D_B} \mathrm{d}x\, \psi_n(x) \psi_m(x), \tag{15}$$

$$F_m \equiv \mu_{1m} \int_{D_A} \mathrm{d}x\, f_1(x) \psi_m(x) + \mu_{2m} \int_{D_B} \mathrm{d}x\, f_2(x) \psi_m(x) \tag{16}$$

as for equation (11), one gets a system of linear equations for the unknown coefficients a_n.

Collocation method. In this method, the residual is forced to zero at N arbitrary points inside the domain D and the a_n coefficients are obtained by solving of the resulting system of linear equations. Then

$$\sum_n a_n \mu_{1n} \psi_n(x_i) - f_1(x_i) = 0, \quad i = 1, \ldots, N_1,\ x \in D_A, \tag{17a}$$

$$\sum_n a_n \mu_{2n} \psi_n(x_i) - f_2(x_i) = 0, \quad i = 1, \ldots, N_2,\ x \in D_B, \tag{17b}$$

with $N = N_1 + N_2$. Solving system (17a)–(17b), one obtains the a_n coefficients.

The points can be chosen in an equidistant way, i.e., by dividing the domain D into N identical intervals:

$$x_i = \frac{i-1}{N-1}, \tag{18a}$$

or in an orthogonal way, where the x_i points are calculated by the formula

$$x_i = \frac{2i-1}{2N-1}. \tag{18b}$$

2.2. DF method

Here we proposed a different technique based on the discretization of unknown functions in the intervals D_A and D_B. The starting point is the pair of dual-series equations (5a) and (5b), for which we have

$$\sum_{n=1}^{N} a_n \mu_{1n} \psi_n(x) = \begin{cases} f_1(x) & \forall x \in D_A, \\ U_2(x) & \forall x \in D_B, \end{cases} \tag{19a}$$

$$\sum_{n=1}^{N} a_n \mu_{2n} \psi_n(x) = \begin{cases} U_1(x) & \forall x \in D_A, \\ f_2(x) & \forall x \in D_B, \end{cases} \tag{19b}$$

where $U_1(x)$ and $U_2(x)$ are unknown functions to be determined.

Now, if we discretize the unknown functions $U_1(x)$ and $U_2(x)$, by dividing the D_A domain into M intervals and the D_B domain into $(N - M)$ intervals, we can approximate

$$U_1(x) \cong p_i, \quad \forall x \in (x_{i-1}, x_i) \equiv d_i^A, \ i = 1, \ldots, M, \tag{20a}$$

$$U_2(x) \cong p_i, \quad \forall x \in (x_{i-1}, x_i) \equiv d_i^B, \ i = M+1, \ldots, N, \tag{20b}$$

where the total number of p_i is N, so that we may rewrite

$$D_A = d_1^A \cup d_2^A \cup \cdots \cup d_M^A, \qquad D_B = d_{M+1}^B \cup d_{M+2}^B \cup \cdots \cup d_N^B.$$

Taking into account equations (20a) and (20b), equations (19a) and (19b) become

$$\sum_{n} a_n \mu_{1n} \psi_n(x) = \begin{cases} f_1(x) & \forall x \in D_A, \\ p_i & \forall x \in d_i^B, \ i = M+1, \ldots, N, \end{cases} \tag{21a}$$

$$\sum_{n} a_n \mu_{2n} \psi_n(x) = \begin{cases} p_i & \forall x \in d_i^A, \ i = 1, \ldots, M, \\ f_2(x) & \forall x \in D_B. \end{cases} \tag{21b}$$

According to equation (21a), the a_n coefficients can be expressed as

$$a_n = \frac{1}{\mu_{1n} Q_n} \left\{ \int_{D_A} \mathrm{d}x\, f_1(x)\psi_n(x) + \sum_{i=M+1}^{N} p_i \int_{d_i^B} \mathrm{d}x\, \psi_n(x) \right\}, \tag{22}$$

where Q_n is the normalization factor, i.e., $Q_n = \int_D \mathrm{d}x\, \psi_n^2(x)$.

Analogously, from equation (21b), the a_n coefficients are calculated as

$$a_n = \frac{1}{\mu_{2n}} \left\{ \int_{D_B} \mathrm{d}x\, f_2(x)\psi_n(x) + \sum_{i=1}^{M} p_i \int_{d_i^A} \mathrm{d}x\, \psi_n(x) \right\}. \tag{23}$$

Finally, by equating (19) to (20), we obtain a system of linear equations, where the N unknown are the values of p_i, i.e.,

$$\sum_{i=M+1}^{N} p_i W_{i,n}^B + \sum_{i=1}^{M} p_i W_{i,n}^A = R_n^B + R_n^A, \tag{24}$$

where

$$W_{i,n}^B = \frac{1}{\mu_{1n}} \int_{d_i^B} \mathrm{d}x\, \psi_n(x), \tag{25a}$$

$$W_{i,n}^A = -\frac{1}{\mu_{2n}} \int_{d_i^A} \mathrm{d}x\, \psi_n(x), \tag{25b}$$

$$R_n^A = -\frac{1}{\mu_{1n}} \int_{D_A} \mathrm{d}x\, f_1(x)\psi_n(x), \tag{25c}$$

$$R_n^B = \frac{1}{\mu_{2n}} \int_{D_B} \mathrm{d}x\, f_2(x)\psi_n(x). \tag{25d}$$

By solving system (24), the calculated p_i values are inserted back into equation (22) (or equation (23)) to find the unknowns a_n.

From equations (21a) and (21b), it is clear that the numerical values of the unknown coefficients a_n depend on the M/N ratio. In all cases we have tested, the best M/N ratio has been found to be $1/3$, even if the W matrix (equations (25a) and (25b)) obtained from this ratio is *less determined*, i.e., it is close to a singular matrix. This problem does not appear when the ratio M/N is $1/2$. In the following, we will name DF1 the solution with the ratio M/N equal to $1/3$ and DF2 the solution with $M/N = 1/2$.

3. Results

3.1. Steady diffusion over an infinite plate

We have applied the DF method to a problem concerning the two-dimensional diffusion equation, which has been carefully studied by Mills and Dudukovic some

years ago [23]. The problem consists in calculating the function that satisfies the Laplace equation:

$$\left[\nabla_x^2 + \nabla_y^2\right] u(x, y) = 0, \quad \forall x \in (0, \pi), \ \forall y > 0, \tag{26}$$

with the conditions

$$u(\pi, y) = P_0, \tag{27a}$$

$$\left.\frac{\partial u(x, y)}{\partial x}\right|_{x=0} = 0, \tag{27b}$$

$$u(x, 0) = 0, \quad 0 < x < c \quad \text{(Dirichelet condition)}, \tag{27c}$$

$$\left.\frac{\partial u(x, y)}{\partial y}\right|_{y=0} = 0, \quad c < x < \pi \quad \text{(Neumann condition)}, \tag{27d}$$

$$u = P_0 \quad \text{as } y \to \infty. \tag{27e}$$

The general solution of equation (26), satisfying conditions (27a), (27b) and (27c) can be written as

$$u(x, y) = P_0 + \sum_n a_n \cos\left[(n - 1/2)x\right] \exp\left[-(n - 1/2)y\right]. \tag{28}$$

Applying the Dirichelet and Neumann conditions, one obtains

$$\sum_n a_n \cos\left[(n - 1/2)x\right] + P_0 = 0, \quad 0 < x < c, \tag{29a}$$

$$\sum_n a_n (n - 1/2) \cos\left[(n - 1/2)x\right] = 0, \quad c < x < \pi. \tag{29b}$$

We solved this pair of dual-series equations (Dini series) by using the analytical solution, our DF1 and DF2 methods, and the MWR methods (embodying the least-square (LS), the Galerkin and the equidistant collocation points (ECP)). In all the calculations, we have set $P_0 = 1$ and $c = \pi/2$.

In figure 2(a), the Neumann condition, equation (29b), is plotted over the entire domain $D \equiv D_A \cup D_B$, with the coefficients a_n obtained by the analytical, DF1 and LS methods, taking into account a limited number of coefficients ($N = 20$). As shown in the figure, the Neumann condition is well reproduced both by DF1 and LS techniques, contrary to the analytical solution which shows a very oscillating behavior for small N. This trend is confirmed by the QSD (quadratic standard deviation, σ^2) of the derivative into the domain D_B ($\pi/2 < x < \pi$), reported in column 6 of table 1. The highest QSD values for the analytical solution indicates a more oscillating behavior in comparison with the DF1 and LS solutions. But the main feature is the smoothness behavior of the DF1 solution in the first domain D_A ($0 < x < \pi/2$). Contrary to the LS and analytical solutions (the first one being much more oscillating), the DF1 solution evidences a much reduced Gibbs effect. As shown in figure 2(b), for high values of N ($= 200$), the analytical and DF1 solutions become almost identical

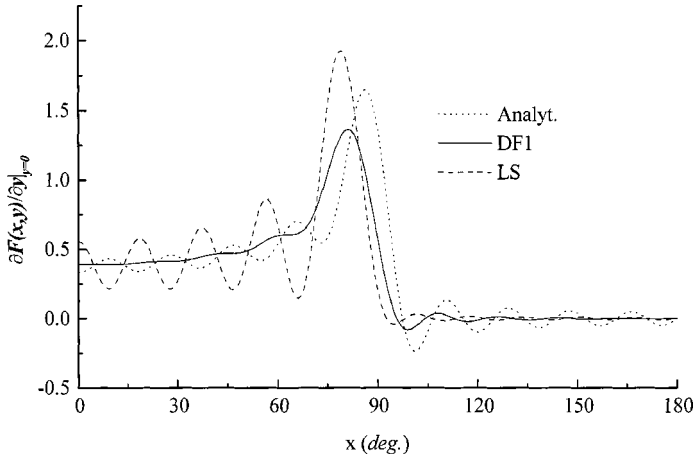

(a)

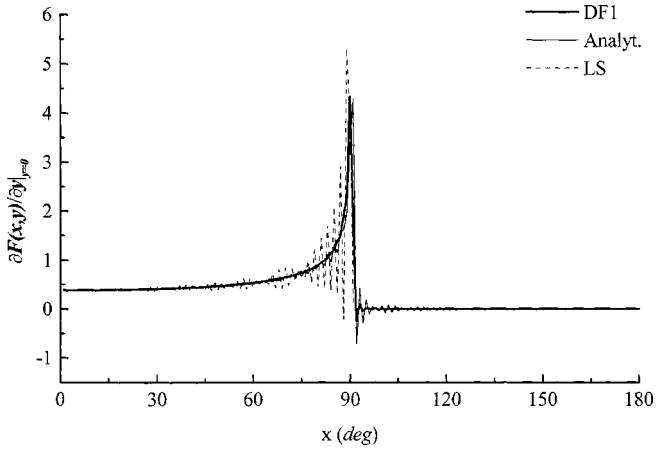

(b)

Figure 2. (a) Dini series: plot of $(\partial F(x,y)/\partial y)|_{y=0}$ over the entire domain $D \equiv D_A \cup D_B$ $(0 < x < 180)$ for $N = 20$ terms of the series. Dotted line: analytical solution, continuous line: DF1 solution, dashed line: least-square solution. (b) The same as in (a), but for $N = 60$ terms of the series.

in the D_A domain, whereas, on increasing the terms of the series, the oscillations of the LS solution increase. In figures 3 and 4 the analytical, the various MWR and the DF1 solutions of equations (29a) and (29b) are compared for $N = 20$ and $N = 60$, respectively. As appears from the figures, the DF1 solution is very smooth in both cases. Exception for the LS technique, which well reproduces the Neumann condition as the DF1 one, the other methods give much more oscillating solutions than those obtained by the DF1 technique. Columns 1–4 of table 1 report the averaged value of equation (29a), $\bar{f}$, and the corresponding QSD for $N = 20$ and $N = 60$. Analogously, columns 5–8 report the averaged value of equation (29b), $\bar{f}'$, together with the corresponding QSD. As far as $\bar{f}$ is concerned, the highest value corresponds

Table 1
Averaged values and quadratic standard deviation of the function into domain D_A (columns 1 and 2) and of its first derivative into domain D_B (columns 3 and 4). The function and its derivative have been calculated at $y = 0$ accounting for 20 and 60 terms in the trigonometric series, respectively.

	$N = 20$		$N = 60$		$N = 20$		$N = 60$	
	$\langle F(x,0)\rangle_{D_A} \equiv \bar{f}$	σ^2	$\langle F(x,0)\rangle_{D_A} \equiv \bar{f}$	σ^2	$\langle \frac{\partial F(x,y)}{\partial y}\vert_{y=0}\rangle_{D_B} \equiv \bar{f}'$	σ^2	$\langle \frac{\partial F(x,y)}{\partial y}\vert_{y=0}\rangle_{D_B} \equiv \bar{f}'$	σ^2
Analyt.	0.00075	0.00008	0.00014	0.00001	0.04227	0.05220	0.02482	0.05338
DF1	0.00870	0.00096	0.00175	0.00012	0.01182	0.00564	0.00687	0.00584
DF2	0.00230	0.00025	0.00046	0.00003	0.01961	0.01974	0.01143	0.02183
LS	0.00190	0.00147	0.00035	0.00029	0.00271	0.00044	0.00055	0.00006
Galer.	0.00560	0.00077	0.00148	0.00014	0.00641	0.00412	0.00145	0.00130
OCP	−0.00074	0.00012	−0.00013	0.00001	0.04308	0.05807	0.02530	0.06726
ECP	0.00130	0.00026	0.00025	0.00003	0.01130	0.02215	0.00640	0.02616

to the DF1 solution indicating that, in spite of the smoothness of the solution, this procedure does not well reproduce the Dirichelet condition near the discontinuity point. This trend can be extracted also from figures 3(a) and 4(a), where the function $F(x, 0)$, calculated by the DF1 procedure, increases starting from 75 ($N = 20$) or 80 ($N = 60$) degrees, at variance of the other methods, where the increase begins near 80 ($N = 20$) or 85 ($N = 60$) degrees. The best $\bar{f}$ is obtained from the analytical, DF2 and OCP solutions, which also determine the best QSD. Similarly, the DF1 method does not well reproduce the Neumann condition near the discontinuity point. Indeed, the calculated values of $\bar{f}'$ indicate that LS and Galerkin solutions are the best approximations, even if the QSDs of the DF1 method suggest the smoothness behavior in comparison with the other methods. Finally, the coefficients a_n calculated by the various techniques for $N = 60$ are plotted in figure 5 as a function of n. It is worth noting the faster convergence of the series calculated by the DF1 procedure with respect to all the other analytical and numerical techniques.

3.2. *Steady diffusion in cylindrical coordinates*

The second problem we have studied is the two-dimensional steady-state diffusion equation in cylindrical coordinates. In this case, the Laplace equation $[\nabla_r^2 + \nabla_z^2]u(r, z) = 0$ is subject to the following conditions:

$$u(r, \infty) = P_0, \tag{30a}$$

$$u(R_0, z) = 0, \tag{30b}$$

$$u(r, 0) = 0, \quad 0 < r < a \quad \text{(Dirichelet condition)}, \tag{30c}$$

$$\left.\frac{\partial u(r, z)}{\partial z}\right|_{z=0} = 0, \quad 0 < r < R_0 \quad \text{(Neumann condition)}. \tag{30d}$$

In the calculations we have set $a = 1$, $P_0 = 1$ and $R_0 = 2$.

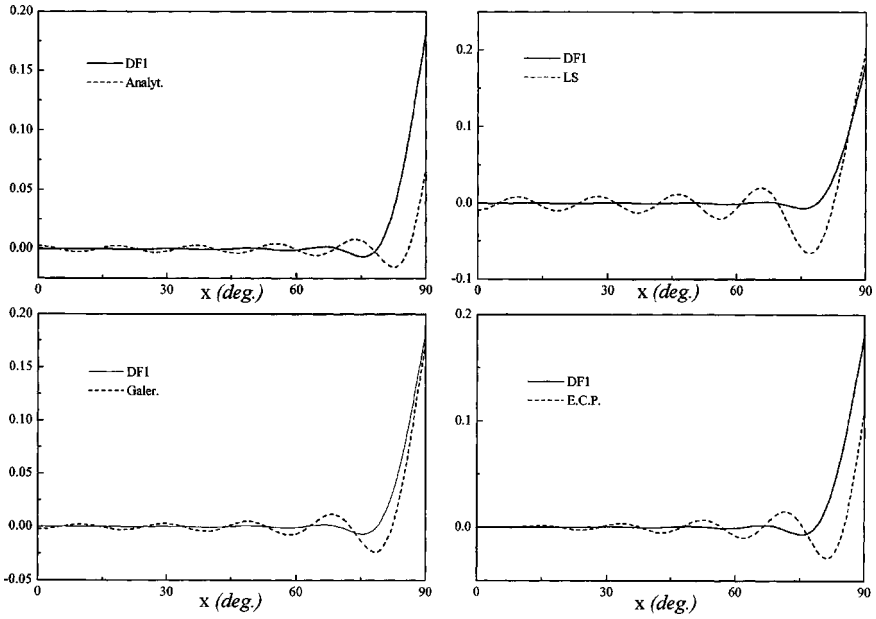

(a)

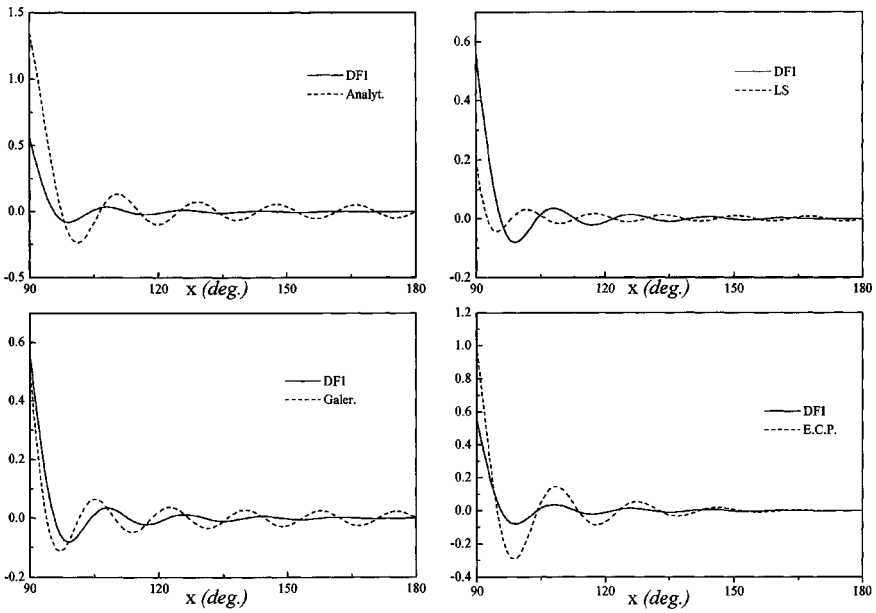

(b)

Figure 3. Dini series: (a) Plot of the Dirichelet condition, $F(x,0)$, over the domain D_A $(0 < x < 90)$ for $N = 20$ terms of the series. (b) Plot of the Neumann condition, $(\partial F(x,y)/\partial y)|_{y=0}$, in the domain D_B $(90 < x < 180)$ for $N = 20$ terms of the series. In each frame, the continuous line represent the DF1 solution, while the dashed lines describe the solutions calculated by other methods, as indicated in the figure.

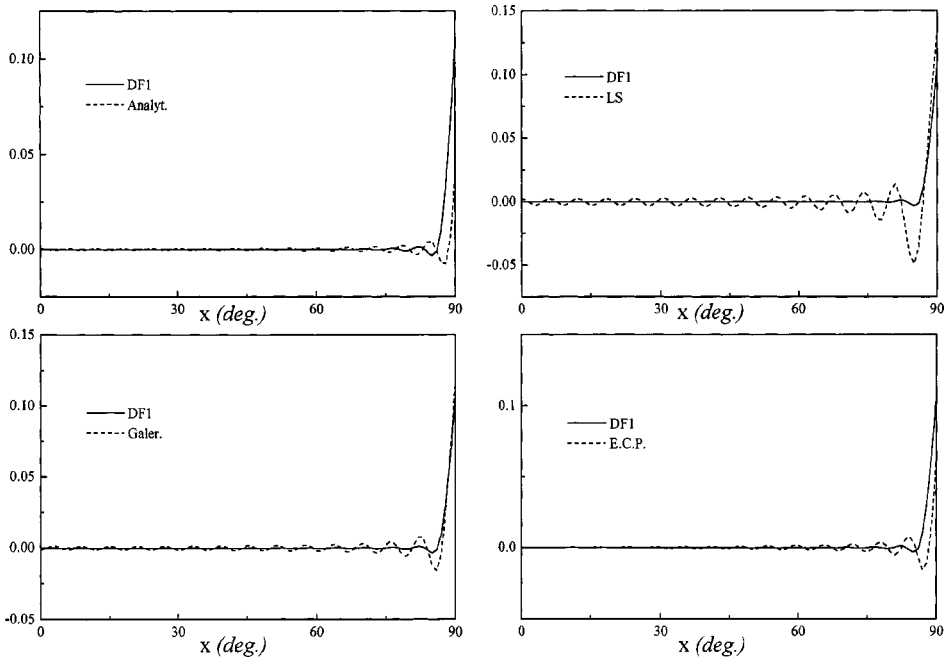

(a)

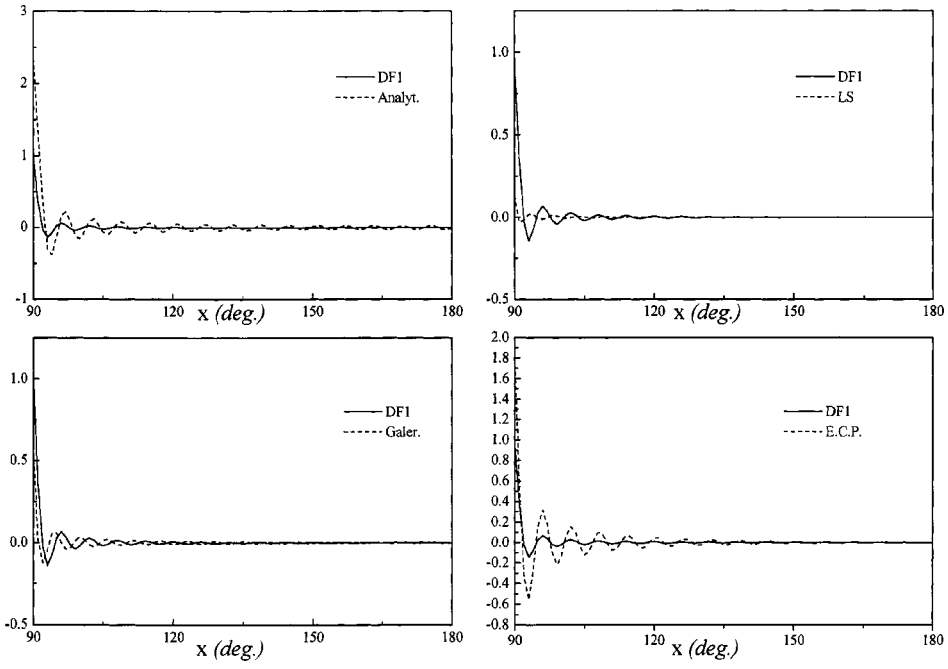

(b)

Figure 4. (a) The same as in figure 3(a), but for $N = 60$ terms of series. (b) The same as in figure 3(b), but for $N = 60$ terms of series.

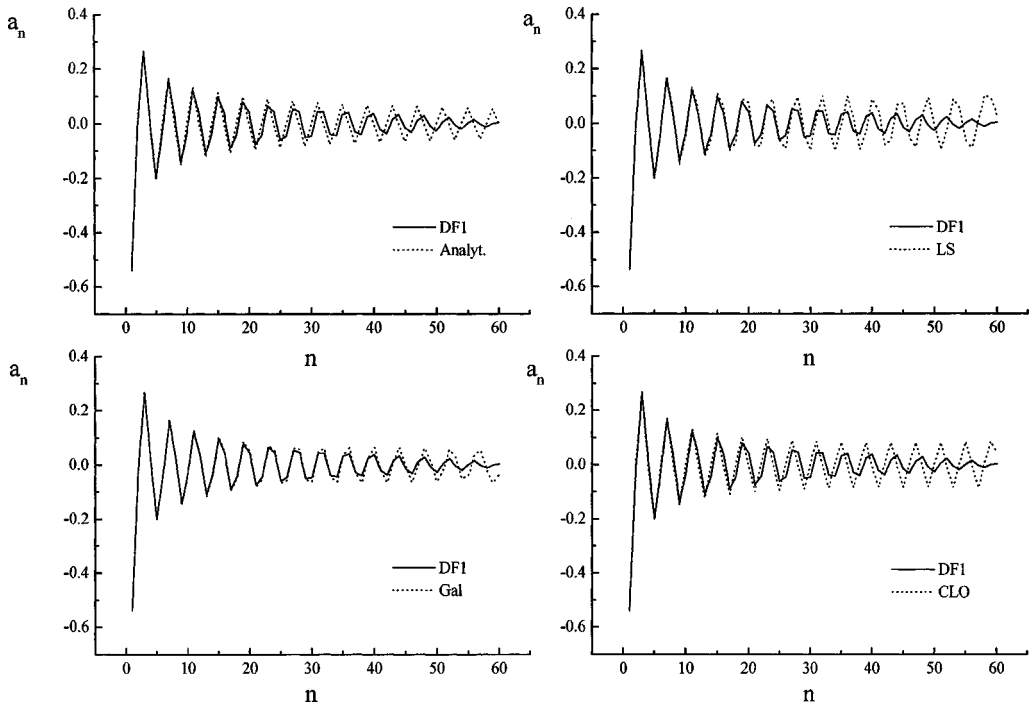

Figure 5. Dini series: plot of the coefficients a_n for $N = 60$ terms of the series. In each frame, the continuous lines represent the DF1 solution, the dashed lines are the solutions calculated by other methods, as indicated in the figure.

The general solution satisfying equations (30a) and (30b) can be written as

$$u(r, z) = P_0 + \sum_n a_n J_0(\lambda_n r) \exp(-\lambda_n z), \tag{31}$$

where $J_0(\lambda_n r)$ is a Bessel function of zero order. Because of the condition (30b), λ_n are the zeros of $J_0(\lambda_n R_0) = 0$.

Applying the Dirichelet and Neumann conditions, we obtain the pair of dual-series equations:

$$u(r, 0) = P_0 + \sum_n a_n J_0(\lambda_n r) = 0, \quad 0 < r < a, \tag{32a}$$

$$\left.\frac{\partial u(r, z)}{\partial z}\right|_{z=0} = -\sum_n a_n \lambda_n J_0(\lambda_n r) = 0, \quad a < r < R_0. \tag{32b}$$

The analytical solution of equations (32a) and (32b) can be found in the book of Sneddon [29]. As for the previous problem, in figure 6 we plot the derivative, equation (32b), over the entire domain D, with the coefficients a_n calculated by analytical, DF1 and LS methods, for $N = 20$. The Neumann condition, equation (30d), is well reproduced both by DF1 and LS techniques, while the analytical solution is much more

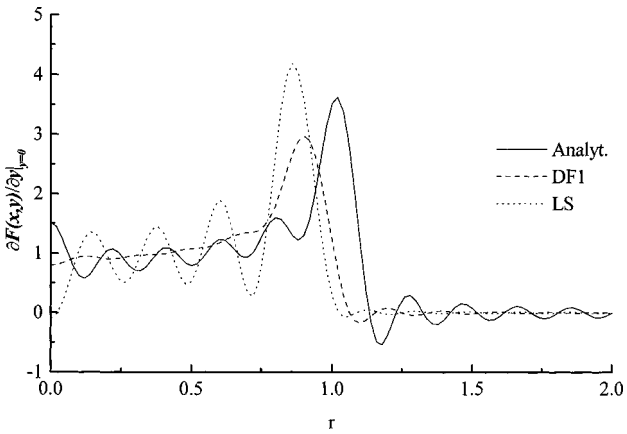

Figure 6. Bessel series: plot of $(\partial F(x,z)/\partial z)|_{z=0}$ over the entire domain $D \equiv D_A \cup D_B$ $(0 < r < 2)$ for $N = 20$ terms of the series. Continuous line: analytical solution, dashed line: DF1 solution, dotted line: least-square solution.

Table 2
As table 1, but for Bessel's series.

	$N = 20$		$N = 60$		$N = 20$		$N = 60$	
	$\langle F(x,0)\rangle_{D_A} \equiv \bar{f}$	σ^2	$\langle F(x,0)\rangle_{D_A} \equiv \bar{f}$	σ^2	$\langle \frac{\partial F(x,y)}{\partial y}\|_{y=0}\rangle_{D_B} \equiv \bar{f}'$	σ^2	$\langle \frac{\partial F(x,y)}{\partial y}\|_{y=0}\rangle_{D_B} \equiv \bar{f}'$	σ^2
Analyt.	−0.00052	0.00003	−0.00002	2.559E−6	−0.28760	−1.00300	−0.20710	−1.19700
DF1	0.01108	0.00158	0.00399	0.00020	−0.02512	−0.02720	−0.01406	−0.02693
DF2	0.00282	0.00042	0.00037	0.00005	−0.04151	−0.09065	−0.02352	−0.09806
LS	0.00376	0.00325	0.00017	0.00061	−0.00185	−0.00050	0.00031	0.00043
Galer.	0.01419	0.00526	−0.00016	0.00038	0.02189	−0.03704	0.00226	−0.03129

oscillating, as confirmed also by the standard deviation values reported in column 6 of table 2. Similarly to the Dini series previously described, the figures show very smooth DF1 solutions in the first domain D_A $(0 < r < 1)$, contrary to the LS and analytical solutions. It could be shown (we have omitted the figure for saving space) that also in this case, the analytical and DF1 solutions coincide inside the D_A domain for high N (=200). On the contrary, on increasing the terms of the series, the oscillations of the LS solution increase. In figures 7 and 8, the analytical and MWR solutions of equations (32a) and (32b) are compared with the DF1 solution for $N = 20$ and $N = 60$, respectively. The curves relative to the collocation methods, OCP and ECP, are not reported because their solutions diverge. It is important to recall that the LS and Galerkin methods require the calculation of integrals like $\int_a^b \rho \, \mathrm{d}\rho \, J_0(\lambda_n \rho) J_0(\lambda_m \rho)$, which are not analytical. We have used a numerical procedure, the Romberg's method [9,19]. Generally, the accuracy of the numerical integration techniques depends on the structure of the integrand function. In this case, the Bessel functions $J_n(x)$ become rapidly oscillating on increasing the index n or, for fixed n, on increasing x. Then, on raising the number of terms of the series, equation (31), the numerical value of the integrals

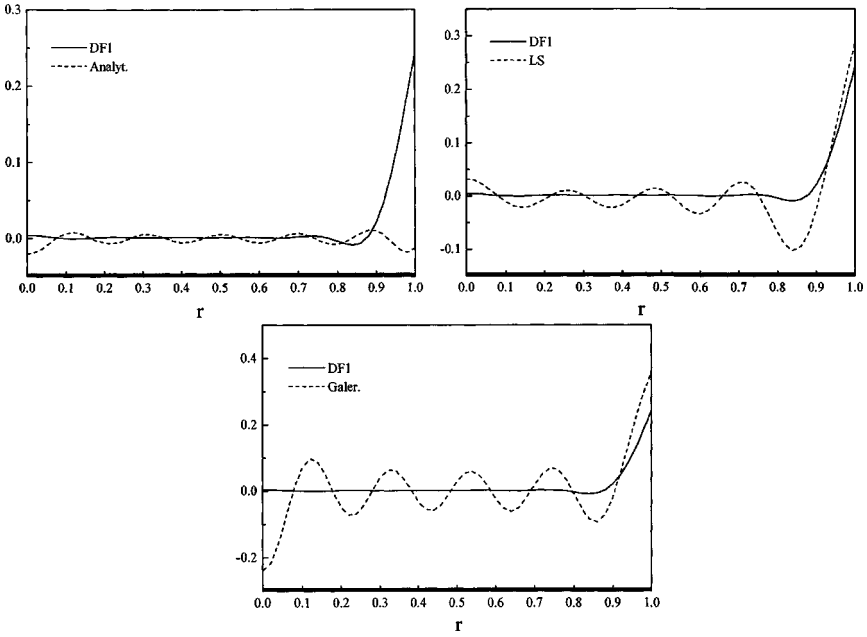

(a)

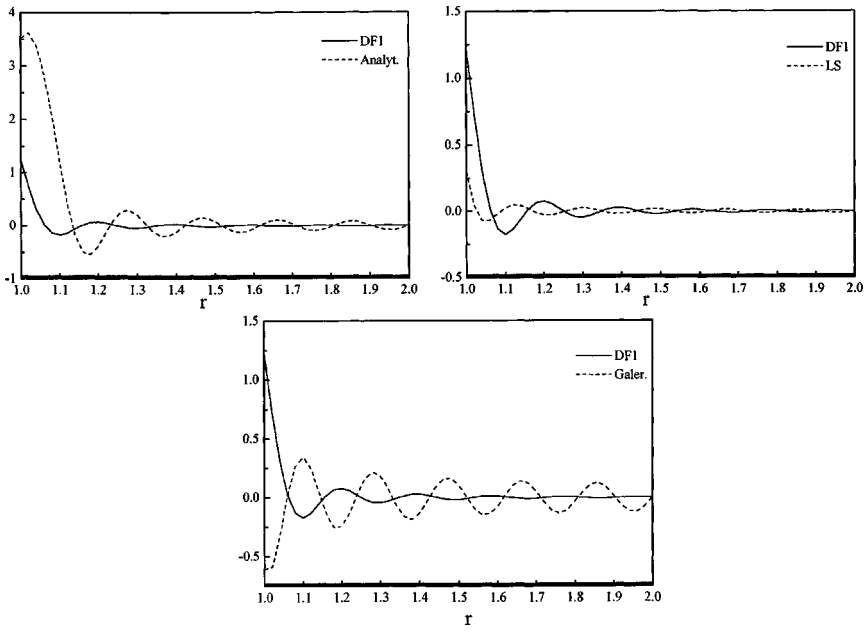

(b)

Figure 7. Bessel series: (a) Plot of the Dirichelet condition, $F(r,0)$, over the domain D_A $(0 < r < 1)$ for $N = 20$ terms of the series. (b) Plot of the Neumann condition, $(\partial F(x,z)/\partial z)|_{z=0}$, over the domain D_B $(1 < r < 2)$ for $N = 20$ terms of the series. In each frame, the continuous lines are the DF1 solution, while the dashed lines are the solutions calculated by other methods, as indicated in the figure.

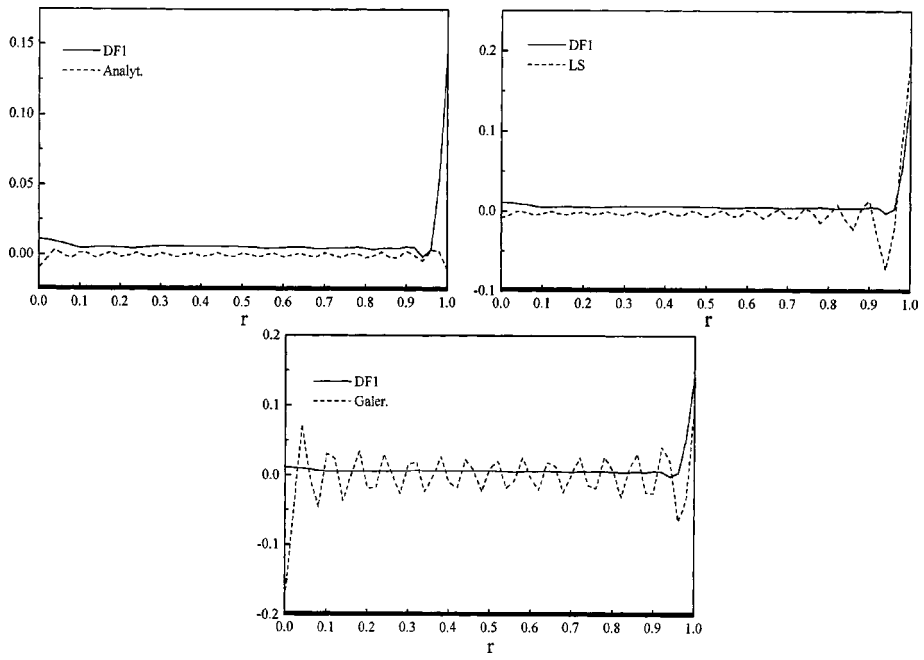

(a)

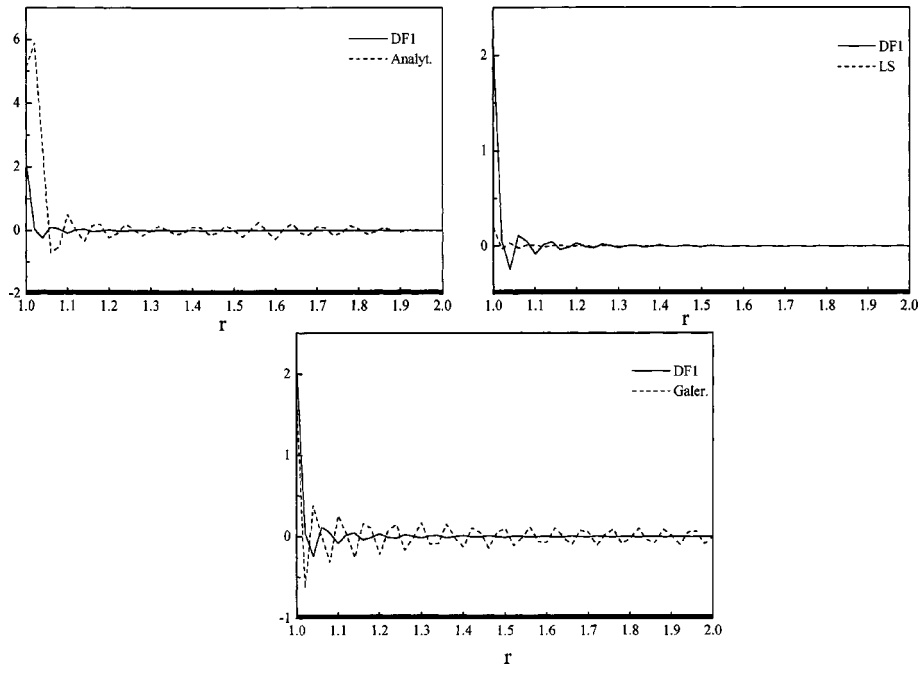

(b)

Figure 8. (a) The same as in figure 7(a), but for $N = 60$ terms of series. (b) The same as in figure 7(b), but for $N = 60$ terms of series.

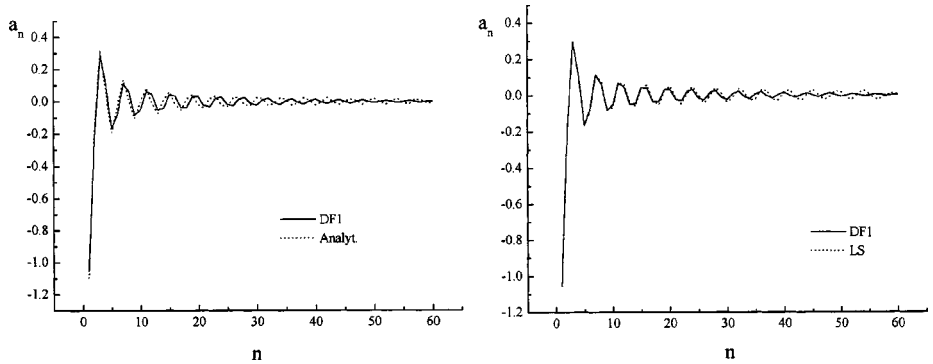

Figure 9. Bessel series: plot of the coefficients a_n for $N = 60$ terms of the series. In each frame, the continuous line represents the DF1 solution, while the dashed lines are the solutions calculated by other methods, as indicated in the figure.

becomes less accurate. It should be possible to improve the accuracy, but this requires a large computational time. As appears from figures 7 and 8, the DF1 solution for both f and f' is very smooth, but on raising the terms of the series, the solution for the Dirichelet condition remains positive over the entire domain D_A. The situation is not improved by inserting many terms of the series, because the LS and the Galerkin methods do not satisfy the Dirichelet condition, probably because of the poor accuracy in the calculation of the integrals. Table 2 reports the mean values and the corresponding QSD. In this case, the DF1 method is not able to contemporary reproduce the Dirichelet and Neumann conditions near the discontinuity. For small terms of the series, the DF2 method better approximates the analytical result for the Dirichelet condition, while the Neumann condition is better approximated by the LS technique. A comparison of the coefficients a_n obtained by the various methods is reported in figure 9 for $N = 60$. The plot of the coefficients as a function of n evidences also in this case a faster convergence for the series calculated by the DF1 technique.

3.3. Steady diffusion in spherical coordinates

Finally, the third problem we have studied is the two-dimensional steady-state diffusion equation in spherical coordinates. In this case, the Laplace equation $[\nabla_\rho^2 + \nabla_\theta^2]u(\rho, \theta) = 0$ is subject to the conditions

$$u(\infty, \theta) = C_0, \tag{33}$$

$$u(R_0, \theta) = 0, \quad 0 < \theta < c \quad \text{(Dirichelet condition)}, \tag{34a}$$

$$\left.\frac{\partial u(\rho, \theta)}{\partial \rho}\right|_{\rho=R_0}, \quad c < \theta < \pi \quad \text{(Neumann condition)}. \tag{34b}$$

In the calculations we have set $c = \pi/2$, $C_0 = 1$ and $R_0 = 1$.

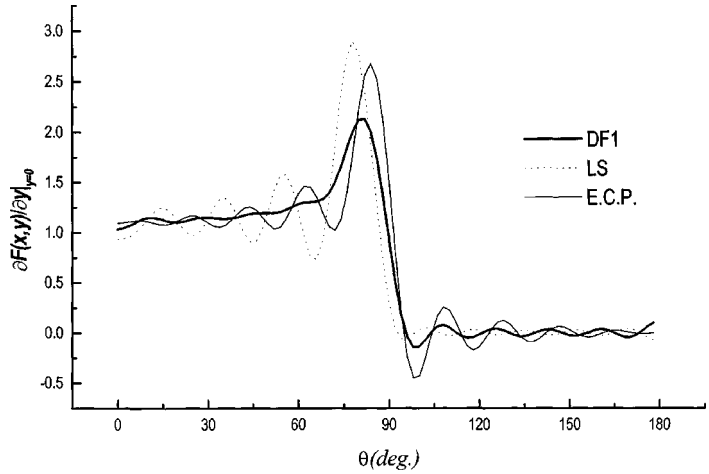

Figure 10. Legendre series: plot of $(\partial F(x,y)/\partial y)|_{y=0}$ over the entire domain $D \equiv D_A \cup D_B$ ($0 < x < 180$) for $N = 20$ terms of the series. Continuous thin line: ECP solution, continuous thick line: the DF1 solution, dotted line: least-square solution.

The general solution of the diffusion equation satisfying condition (33) is

$$u(\rho,\theta) = C_0 + \sum_n \frac{a_n}{\rho^{n+1}} P_n(\cos\theta), \tag{35}$$

where $P_n(\cos\theta)$ are Legendre polynomials.

Applying the Dirichelet and Neumann conditions, we obtain the pair of dual-series equations:

$$u(\rho,\theta) = C_0 + \sum_n a_n P_n(\cos\theta) = 0, \quad 0 < \theta < c, \tag{36a}$$

$$\left.\frac{\partial u(\rho,\theta)}{\partial \rho}\right|_{\rho=R_0} = -\sum_n a_n (n+1) P_n(\cos\theta) = 0, \quad c < \theta < \pi. \tag{36b}$$

The analytical solution of the pair of equations (36a) and (36b) is unknown. Therefore, we have solved equations (36) by the DF1, DF2, LS, Galerkin and collocation point methods. As for the previous cases, in figure 10 we plot equation (36b) over the entire domain $D = D_A \cup D_B$, with the coefficient a_n obtained by the DF1, LS and ECP methods for $N = 20$. The smoothness of the function into the first domain ($0 < \theta < \pi/2$) calculated by the DF1 approximation, is noticeable even in spherical coordinates, indicating that this feature is intrinsic of the DF1 technique and independent of the type of coordinates employed in the calculations. Figures 11 and 12, which report the Dirichelet and Neumann conditions calculated with $N = 20$ and $N = 60$, show that the Dirichelet condition is well reproduced by DF1, DF2 and ECP techniques, the solutions corresponding to the DF1 method being less oscillating. Also in this case, the Neumann condition is better reproduced by the LS method, even if the DF1 and

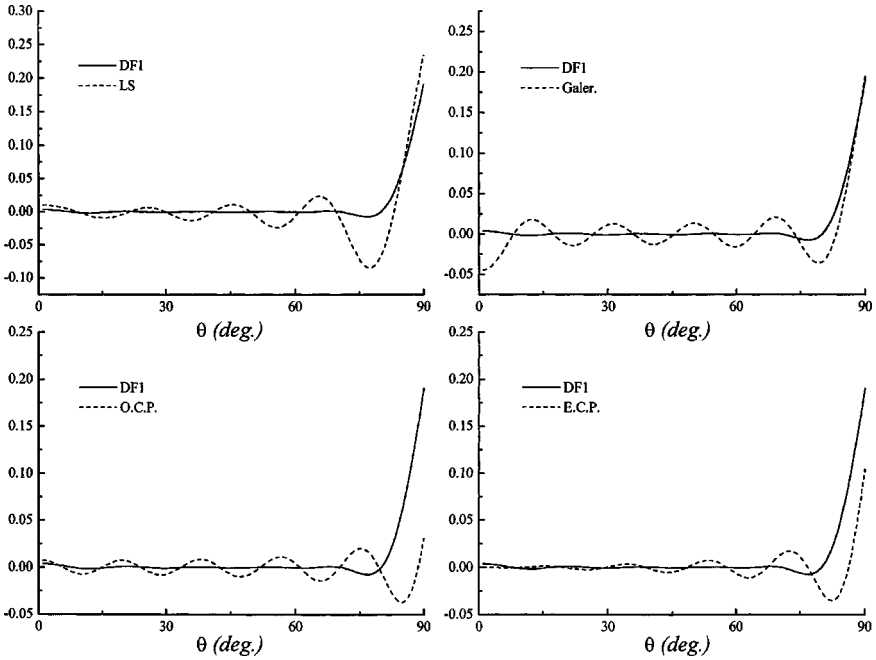

(a)

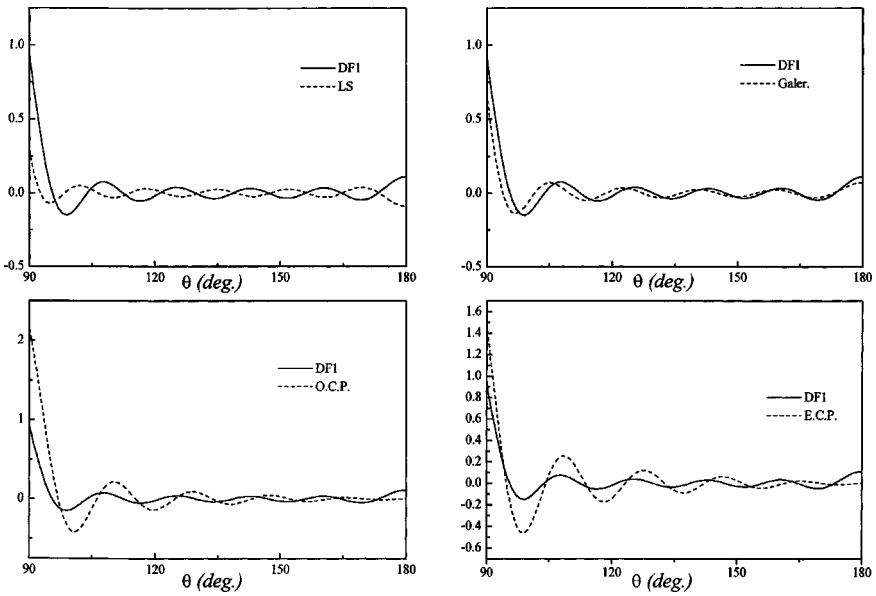

(b)

Figure 11. Legendre series: (a) Plot of the Dirichelet condition, $F(x,0)$, over the domain D_A ($0 < x < 90$) for $N = 20$ terms of the series. (b) Plot of the Neumann condition, $(\partial F(x,y)/\partial y)|_{y=0}$, over the domain D_B ($90 < x < 180$) for $N = 20$ terms of the series. In each frame, the continuous line is the DF1 solution, while the dashed lines are the solutions calculated by other methods, as indicated in the figure.

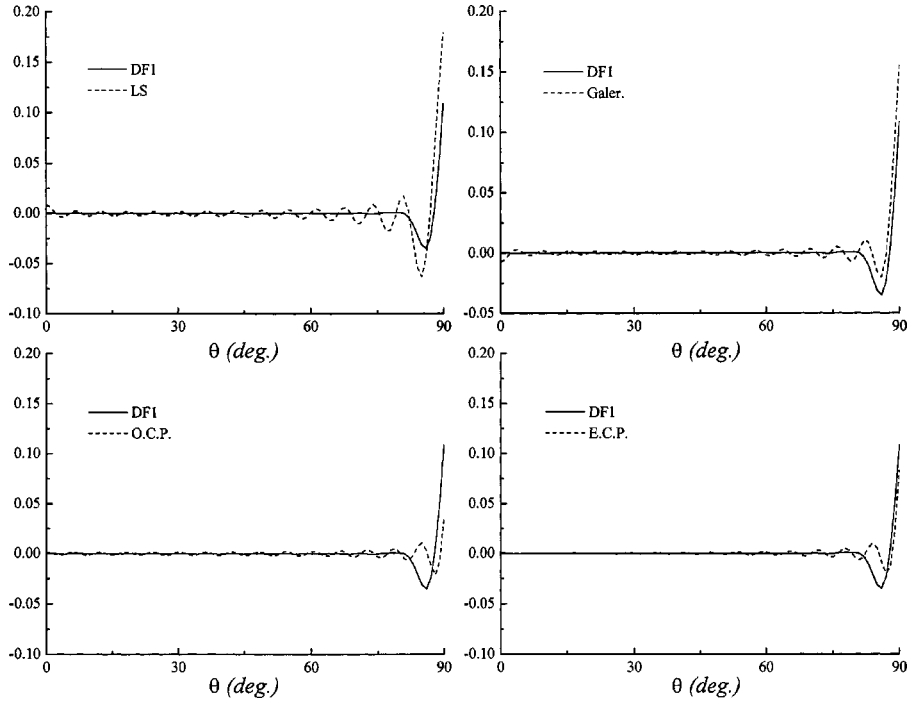

(a)

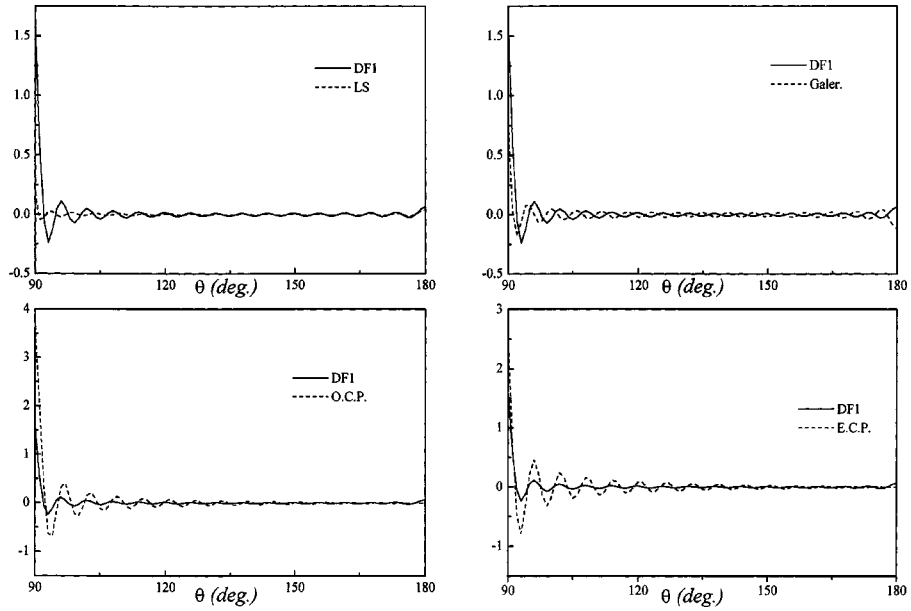

(b)

Figure 12. (a) The same as in figure 11(a), but for $N = 60$ terms of series. (b) The same as in figure 11(b), but for $N = 60$ terms of series.

Table 3
As table 1, but for Legendre's series.

	$N = 20$		$N = 60$		$N = 20$		$N = 60$	
	$\langle F(x,0)\rangle_{D_A} \equiv \bar{f}$	σ^2	$\langle F(x,0)\rangle_{D_A} \equiv \bar{f}$	σ^2	$\langle \frac{\partial F(x,y)}{\partial y}\vert_{y=0}\rangle_{D_B} \equiv \bar{f}'$	σ^2	$\langle \frac{\partial F(x,y)}{\partial y}\vert_{y=0}\rangle_{D_B} \equiv \bar{f}'$	σ^2
DF1	0.01002	0.00137	−0.00018	0.00012	0.0188	0.01584	0.01117	0.01575
DF2	0.00293	0.00038	0.00059	0.00005	0.02751	0.04471	0.01550	0.04256
LS	0.00374	0.00265	0.00064	0.00051	0.00374	0.00107	0.00064	0.00013
Galer.	0.00754	0.00146	0.00198	0.00024	0.00754	0.00644	0.00198	0.00263
OCP	−0.00093	0.00014	−0.00017	0.00002	0.06201	0.1256	0.03462	0.12840
ECP	0.00172	0.00039	0.00032	0.00004	0.01637	0.05353	0.00878	0.05195

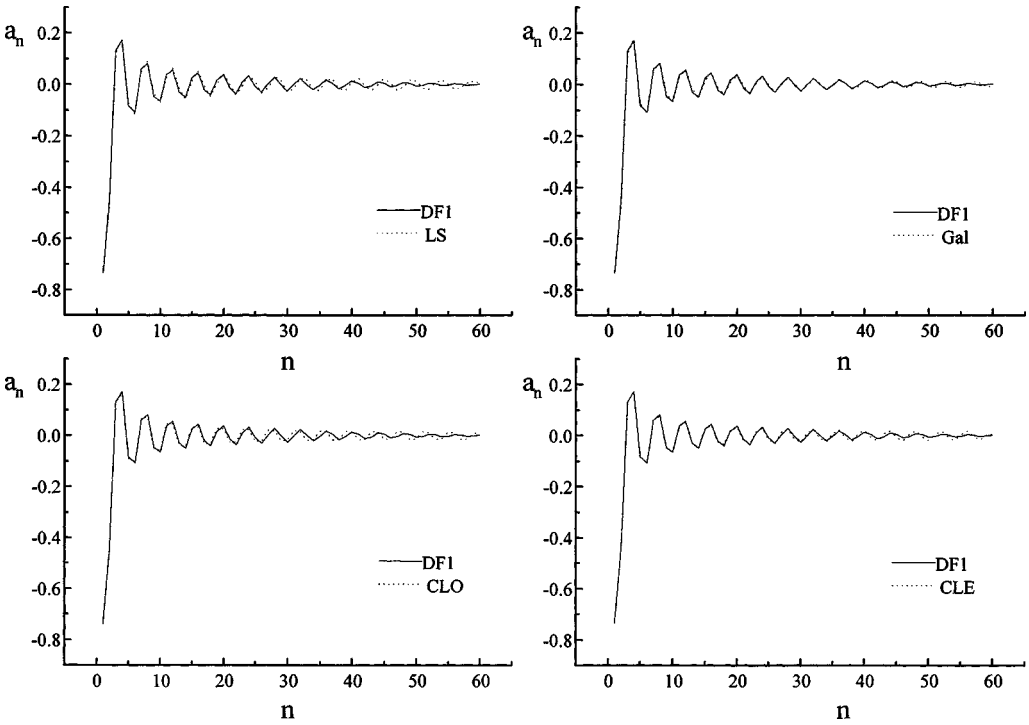

Figure 13. Legendre series: plot of the coefficients a_n for $N = 60$ terms of the series. In each frame, the continuous line is the DF1 solution, while the dashed lines are the solutions calculated by other methods, as indicated in the figure.

Galerkin solutions have a comparable accuracy. The mean values of the function f, reported in table 3, indicate that for small N, the collocation point, the DF1 and ECP methods (this latter only for high N) give the best results both for $\bar{f}$ and its QSD, while the LS and Galerkin methods give the best results both for $\bar{f}'$ and the corresponding QSD. Unfortunately, also in spherical coordinates the DF1 procedure is not able to contemporary reproduce the two conditions near the discontinuity. Finally, a comparison of the series coefficients a_n obtained by the various methods, for $N = 60$,

is reported in figure 13. The plot of a_n as a function of n evidences also in this case a faster convergence for the series calculated by the DF1 technique.

4. Conclusions

In this paper, we have developed a new numerical method to solve the general problem of MBCs. This approach, based on the discretization of unknown functions (DF), has been applied to MBCs problems expressed in different coordinate systems (trigonometric, cylindrical and spherical) and has been compared with existing numerical methods as well as with the analytical solution (when available). The new method reveals to be the most efficient one in solving MBCs problems in all coordinate systems. In fact, our procedure can be applied to problems involving series of Bessel's function, as the well-known LS and Galerkin methods, where the collocation points technique fails. The DF technique gives a good approximation of the exact solution for both Dirichelet and Neumann conditions, while the LS and Galerkin methods, which reproduce very well the Neumann condition, are worse approximations for the Dirichelet condition. Moreover, all the integrals contained in the DF procedure are analytical, whereas other procedures (e.g., LS and Galerkin) require integrals containing product of functions, which in some cases (as in the case of Bessel's functions) are not analytical and must be numerically solved, with a loss of accuracy and an increase of the calculation time. However, the main features of our procedure are twofold: (a) a very fast convergence of the resulting series; (b) the very smooth behavior of the function and of the derivative function throughout the entire domain D, even for a small number of terms in the series, whereas other methods, including the analytical, show oscillating solutions, unless a very large number of terms are considered. The only drawback of the DF approach is its behavior near the discontinuity point. Because of this limit, the mean values calculated for the Dirichelet and Neumann conditions look in some cases less accurate than those calculated by other methods.

Concluding, we believe that the DF approximation can be inserted in a list of very efficient numerical techniques usable to solve MBCs problems. Finally, starting from the DF approach it is possible to develop other numerical procedures by combining together the techniques typical of DF and weighted residual methods. Work is in progress along this line.

Acknowledgements

We are very grateful to Dr. P.L. Mills (Dupont Central Research and Development) for his useful suggestions and comments. We are also grateful to Professor M.P. Dudukovic (Department of Chem. Eng., Washington University) for his courtesy. This work was supported by MURST (40% and 60%) and by CNR.

References

[1] U.S. Agarwal and D.V. Khakas, J. Chem. Phys. 96 (1992) 7152.
[2] M. Baldo, A. Grassi, G.M. Lombardo and A. Raudino, J. Chem. Phys. 105 (1996) 8404.
[3] M. Baldo, A. Grassi and A. Raudino, J. Chem. Phys. 91 (1989) 4658.
[4] M. Baldo, A. Grassi and A. Raudino, Phys. Rev. A 39 (1989) 3700.
[5] M. Baldo, A. Grassi and A. Raudino, Phys. Rev. A 40 (1989) 1017.
[6] M. Baldo, A. Grassi and A. Raudino, J. Chem. Phys. 93 (1990) 6034.
[7] M. Baldo, A. Grassi and A. Raudino, J. Phys. Chem. 95 (1991) 6734.
[8] M. Baldo, A. Grassi and A. Raudino, J. Math. Phys. 33 (1992) 2329.
[9] B. Carnahan, H.A. Luther and J.O. Wilkes, *Applied Numerical Methods* (Wiley, New York, 1969).
[10] C. Chu and K. Chon, J. Catal. 17 (1970) 71.
[11] J. Crank, *The Mathematics of Diffusion* (Clarendon, Oxford, 1970).
[12] C. DeLisi, in: *Cell Surface Dynamics*, eds. A.S. Perelson, C. DeLisi and F.W. Wiegel (Dekker, New York, 1984) p. 135.
[13] M.P. Dudukovic and P.L. Mills, in: *Proc. 5th Int. Symp. Chem. React. Engng.*, ACS Symp. Ser., Vol. 65 (1978) p. 387.
[14] B.A. Filayson, Br. Chem. Eng. 14 (1969) 53.
[15] A. Grassi and A. Raudino, J. Phys. Chem. 100 (1996) 16934.
[16] R.B. Kelman, J. Math. Phys. 46 (1967) 333.
[17] R.B. Kelman, Quart. J. Mech. Appl. Math. 23 (1970) 549.
[18] H. Levine, Appl. Sci. Res. 39 (1982) 261.
[19] J.H. Mathews, *Numerical Methods for Mathematics, Science and Engineering*, 2nd ed. (Prentice-Hall, NJ, 1992).
[20] W.W. Mayer, L.L. Hegedus and R.K. Aris, J. Catal. 42 (1976) 135.
[21] J.A. McCammon, R.J. Bacquet, S.A. Allison and S.H. Northrup, Faraday Discuss. Chem. Soc. 83 (1987) 213.
[22] P.L. Mills and M.P. Dudukovic, Ind. Eng. Chem. Fund. 18 (1978) 129.
[23] P.L. Mills and M.P. Dudukovic, Chem. Eng. Sci. 35 (1980) 1557.
[24] P.L. Mills and M.P. Dudukovic, Comput. Chem. Eng. 6 (1982) 141.
[25] P.L. Mills and M.P. Dudukovic, Math. Modelling 5 (1984) 171.
[26] P.L. Mills, S.S. Lai and M.P. Dudukovic, Ind. Eng. Chem. Fund. 24 (1985) 64.
[27] P.A. Ramachandran and J.M. Smith, AIChE J. 25 (1979) 538.
[28] D. Shoup, G. Lipari and A. Szabo, Biophys. J. 36 (1981) 697.
[29] I.N. Sneddon, *Mixed Boundary Value in Potential Theory* (North-Holland, Amsterdam, 1966).
[30] A. Szabo, D. Shoup, S.H. Northrup and J.A. McCammon, J. Chem. Phys. 77 (1982) 4484.
[31] S.D. Traytak, J. Phys. Chem. 98 (1994) 7419.
[32] J.V. Villadsen and M.L. Michelsen, *The Method of Weighted Residual and Variational Methods* (Academic Press, New York, 1972).
[33] J.V. Villadsen and M.L. Michelsen, *Solution of Differential Equation Models by Polynomial Approximation* (Prentice-Hall, NJ, 1978).
[34] J.V. Villadsen and W.E. Stewart, Chem. Eng. Sci. 22 (1967) 1967.
[35] J.R. Whiteman and J.C. Webb, Nordish Tidskr. Informations Behandling (BIT) 10 (1970) 366.
[36] F.W. Wiegel, Phys. Rep. 95 (1983) 283.
[37] F.W. Wiegel, in: *Cell Surface Dynamics*, eds. A.S. Perelson, C. DeLisi and F.W. Wiegel (Dekker, New York, 1984) p. 135.
[38] H.A. Wilson, Proc. Cambridge Philos. Soc. 12 (1904) 406.
[39] H.X. Zhou and A. Szabo, J. Phys. Chem. 100 (1996) 2597.
[40] D. Zwillinger, *Handbook of Differential Equations* (Academic Press, New York, 1989).